Adsorption of tranexamic acid on hydroxyapatite: Toward the development of biomaterials with local hemostatic activity

Stéphanie Sarda, Farid Errassifi, Olivier Marsan, Anne Geffre, Catherine Trumel, Christophe Drouet

Adsorption of tranexamic acid on hydroxyapatite: Toward the development of biomaterials with local hemostatic activity

Stéphanie Sarda [a,*], Farid Errassifi [a], Olivier Marsan [b], Anne Geffre [c,d], Catherine Trumel [c,d], Christophe Drouet [b]

[a] CIRIMAT, Université de Toulouse, CNRS, INPT, UPS, Université Toulouse 3 Paul Sabatier, Toulouse, France
[b] CIRIMAT, Université de Toulouse, CNRS, INPT, UPS, ENSIACET, Toulouse, France
[c] Université de Toulouse, INP, ENVT, UMS006, Laboratoire Central de Biologie Médicale, Toulouse, France
[d] INSERM-UPS, UMS 006, Laboratoire Central de Biologie Médicale, Toulouse, France

ARTICLE INFO

Keywords:
Hydroxyapatite
Tranexamic acid
Hemostatic agent
Adsorption
Release

ABSTRACT

This work proposes to combine *tranexamic acid (TAX)*, a clinically used antifibrinolytic agent, and hydroxyapatite (HA), widely used in bone replacement, to produce a novel bioactive apatitic biomaterial with intrinsic hemostatic properties. The aim of this study was to investigate adsorptive behavior of the TAX molecule onto HA and to point out its release in near physiological conditions.
No other phase was observed by X ray diffraction or transmission electron microscopy, and no apparent change in crystal size was detected. The presence of TAX on the powders was lightly detected on Raman spectra after adsorption. The adsorption data could be fitted with a Langmuir Freundlich equation, suggesting a strong interaction between adsorbed molecules and the formation of multilayers. The concentration of calcium and phosphate ions in solution remained low and stable during the adsorption process, thus ion exchange during the adsorption process could be ruled out. The release of TAX was fast during the first hours and was governed by a complex process that likely involved both diffusion and dissolution of HA. Preliminary aPTT (activated partial thromboplastin time) hemostasis tests offered promising results for the development of osteoconductive apatitic biomaterials with intrinsic hemostatic properties, whether for dental or orthopedic applications.

1. Introduction

Orthopedic, dental, and trauma surgeries are accompanied, among others, by a high risk of bleeding, and uncontrolled hemorrhage can be the leading cause of blood transfusions, morbidity, and mortality. Blood transfusions may be a life saving measure in such cases, but it remains an expensive resource and can result in a variety of problems for patients like the risk of infection transmission.

Hemostasis is defined as "the stoppage of bleeding." The three major steps of hemostasis are 1.) *vasoconstriction*, which diminishes blood loss; 2.) *exposure of collagen*, which initiates a series of reactions called the coagulation cascade on the wall of blood vessels, leading to the formation of a primary hemostatic plug; and finally, 3.) *adhesion of platelets* onto the blood vessel wall, leading to the conversion of fibrinogen into fibrin to create the final clot [1]. Effective and rapid hemostasis is critical to optimize surgical outcomes. In this context, hemostatic agents are adjuvants used in surgery to improve hemostasis when conventional techniques (clips, staples, sutures, ligatures, and electrocoagulation) are insufficient [2]. Various hemostatic drugs have thus been used and show some efficacy in many types of surgery [3].

Tranexamic acid [*trans* 4 (aminomethy1) cyclohexanecarboxylic acid, TAX] is a clinically used antifibrinolytic agent (Fig. 1). It is a synthetic lysine analog and is used to manage of different bleeding disorders as well as to reduce postoperative blood loss in patients undergoing high bleeding risk surgeries. The hemostatic property of TAX mainly relates to its ability to inhibit the conversion of plasminogen to plasmin, thereby preventing excessive blood loss in hyperfibrinolytic conditions. Plasmin breaks down fibrinogen and a series of other proteins involved in coagulation [3,4]. TAX however presents a low bioavailability of only 30 50% by oral administration [5]. In orthopedic surgery such as knee or hip arthroplasty, TAX appears to be more efficacious when a dose of >30 mg/kg is used [4]. Moreover, it has been found to cause gastrointestinal side effects when administered orally, whereas this has not been reported with intravenous administration. However, rapid intravenous boluses may cause hypotension, so it is recommended that it is given either over 10 min or via infusion, although its dose needs to be reduced in cases of renal impairment. Thus, especially for surgical procedures known to present a high risk for bleeding, the search for improved hemostasis approaches or methodologies is still undergoing.

One appealing approach when dealing with bone related surgeries is to confer hemostatic properties to the implanted biomaterial itself. Calcium phosphates with an apatitic structure (apatites) constitute the mineral part of calcified tissues such as bone and teeth [6] and are for this reason widely used for bone related biomedical applications,

* Corresponding author at: CIRIMAT, INPT-CNRS-UPS, Université de Toulouse, Université Paul Sabatier, 4 Allée Emile Monso, BP 44362, 31030 Toulouse Cedex 04, France.
E-mail address: stephanie.sarda@iut-tlse3.fr (S. Sarda).

http://dx.doi.org/10.1016/j.msec.2016.04.032

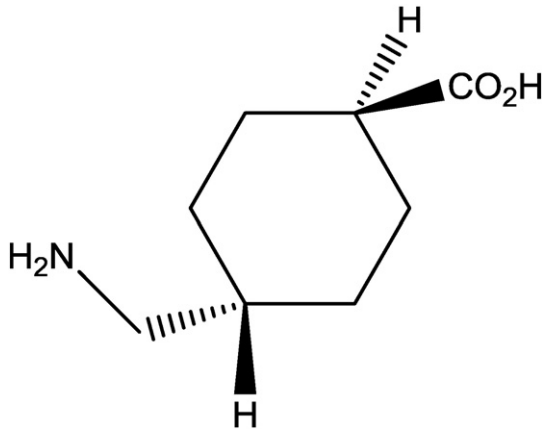

Fig. 1. Tranexamic acid (TAX).

in various forms including powders, scaffolds, self setting cements, or coatings [7,8]. Surface functionalization of apatite crystals with biomol ecules of biological interest (e.g., growth factors, drugs, enzymes, etc.) also increases its potential for medical uses: for example, in the field of bone repair, for activating bone tissue regeneration, for limiting oste oclastic resorption, or preventing bone infections. Due to their excep tional surface reactivity, apatitic compounds have been widely studied with drug delivery objectives [9]. Adsorption on apatitic surfaces (as op posed to simple impregnation) leads to a stable association and control of the amount of bioactive molecules associated in the solid implant, and thus of the dose released, that increase its potential for the develop ment of osteoconductive biomaterials with drug delivery properties [10]. Also, the understanding of biomineralization events involves a bet ter comprehension of biomolecules adsorption phenomena. For in stance, several bone proteins such as osteocalcin, osteopontin, as well as biomolecules including albumin, or else phospholipids, among others, have been shown to adsorb strongly onto apatite [11,12]. In the biomaterials field, some bone adsorbing molecules used in the treatment of bone diseases, like bisphosphonates, have been used to control bone turnover and their biological activity has been shown to correlate with their adsorption properties [9]. The surface characteris tics of apatites are also largely used in separation chromatography of proteins, and in fact, preparatory and development studies for these ap plications have initiated research on adsorption on apatite surface [13].

Among the calcium phosphate compounds widely used nowadays in bone replacement, stoichiometric hydroxyapatite (HA, $Ca_{10}(PO_4)_6(OH)_2$) is the most commonly found. The aim of this work was to combine TAX and hydroxyapatite to produce a novel bioactive apatitic biomaterial with intrinsic hemostatic properties. Such biomaterials may be used in orthopedic or dental surgery to control blood loss while avoiding the ad verse effects of systemic medication. The adsorption of TAX on HA could allow controlling the release of the hemostatic drug. Thus, the aim of this study was in priority to investigate the adsorptive behavior of TAX onto HA and to point out its release in near physiological conditions. Full char acterizations of the powders before and after adsorption were also per formed to better understand the mechanism of adsorption.

2. Materials and methods

2.1. Materials

Stoichiometric hydroxyapatite (HA) was synthesized by double de composition by adding dropwise a phosphate salt aqueous solution (1.54 M $(NH_4)_2HPO_4$, 433.3 mL) into a calcium salt aqueous solution (1 M $Ca(NO_3)_2.4H_2O$, 1100 mL) at 90 °C under continuous stirring [14]. The pH of the suspension during the synthesis was approximately 10 by adding NH_4OH. After filtration, the precipitate was washed and freeze dried. The powder obtained was sieved (<125 μm) and stored in a freezer.

The phosphate content in the HA sample was determined by spectrophotometry using the phosphovanadomolybdic acid complex method and the calcium content was measured by complexometry with EDTA (relative error of 0.5%) [15]. The determination of the atomic Ca/P ratio of the precipitate was reached with a relative error of 1%. The specific surface area of the powder was determined by nitrogen adsorp tion according to the Brunauer Emmett Teller (BET) method with a Quantachrome Instruments Monosorb NOVA 1000.

Powder of tranexamic acid (*trans* 4 (aminomethy1)cyclohexanecar boxylic acid, TAX) was obtained from Sigma Aldrich (purity 97%). *Cis* 4 (aminomethyl)cyclohexanecarboxylic acid was used as the internal standard (IS) for TAX titration and was purchased from Sigma Aldrich (purity 95%).

2.2. Adsorption experiments

Adsorption experiments were performed in 1 mM potassium chlo ride aqueous solution of TAX (initial concentration varied from 0 to 6 g/L or 3.8×10^{-2} M). 50 mg of the HA sample was dispersed in 5 mL of the adsorption medium in a polypropylene tube and sonicated for a few minutes (initial pH about 7.2). Preliminary tests demonstrated that the kinetics of adsorption of TAX on HA was slow; therefore, the suspensions obtained were incubated in the presence of TAX for 24 h (without stirring and at ambient temperature). After incubation, the ad sorption tubes were centrifuged for 20 min at 5000 rpm. The resulting supernatants were filtered through Millipore filters (pore size 0.2 μm) and analyzed for calcium and phosphate titrations. The solids (HA TAX) retrieved after adsorption were freeze dried and stored in a freez er before characterization. Blanks containing only the adsorption solu tion incubated without solid were used as controls.

2.3. Solution analysis

Phosphate and calcium levels in the supernatants were determined by Inductively Coupled Plasma Atomic Emission Spectroscopy (ICP OES, Horiba Jobin Horibo).

There is no chromophore in the TAX molecule enabling direct anal ysis by UV visible spectrophotometry. Therefore, TAX was titrated in solution using a liquid chromatography/mass spectrometry (LC/MS) method previously adapted from Grassin *et al.* [16]. Chromatographic separation was performed on a 6140 Quadrupole 1200 Series LC system using an Uptisphere® Strategy™ C18 2 Column (5 μm, 4.6 × 150 mm, Agilent Technologies). The mobile phase was prepared by adjusting formic acid solution (0.1%) and methanol in the ratio 48:52 (*v*/v). The flow rate was 5 μL/s, the run time was equal to 4 min and the injection volume was 10 μL. A peak was observed at 2.29 min for TAX and 2.30 for IS. A mass spectrometer, equipped with an electrospray ionization (ESI) source was used for detection and quantification.

Stock solutions of TAX (1 g/L) and of the internal standard (IS, 0.4 g/L) were prepared separately in ultra pure water. TAX (from 0 to 12 ppm) and IS (5 ppm) calibration samples were prepared in triplicate by dilution of their stock solutions in ultra pure water. The calibration curve (Fig. 2) was obtained by plotting the peak area ratio of TAX to IS (TAX/IS) as a function of TAX concentration. The calibration equation was obtained by linear regression analysis ($r^2 = 0.9997$).

2.4. Release kinetics

TAX release profiles were obtained with a flow through cell system (USP Apparatus 4, Sotax AG, Switzerland) with a ø = 12 mm cell (6 mL) and a piston pump (Sotax CY, Sotax AG, Switzerland). Release tests were performed at 37.0 ± 0.5 °C under sink conditions according to the European Pharmacopoeia guidelines [17]. The dissolution medium consisted of ultra pure water pumped through the column at a flow

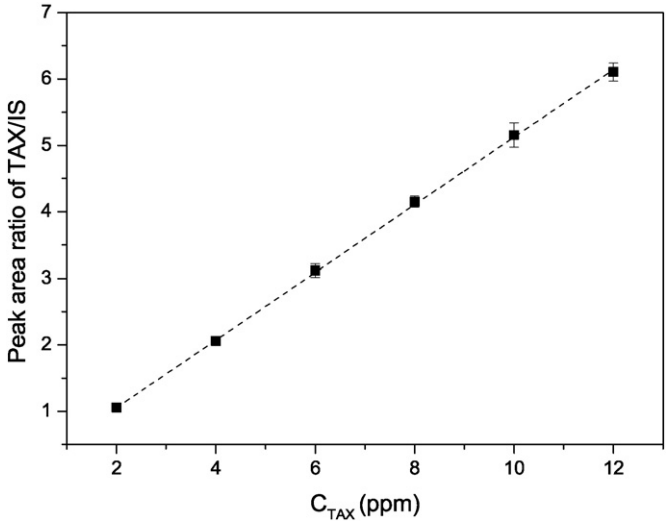

Fig. 2. Calibration curve of tranexamic acid by LC/MS method.

rate of 15 mL/min and the closed system consisted of 50 mL of recycled dissolution medium. In all experiments, laminar flow was used with a bed of 1 g of glass beads covered with 100 mg of HA powder after TAX adsorption (175 μmol TAX/g HA).

Periodically, 5 mL of dissolution medium was collected and filtrated through Millipore filters (pore size 0.2 μm) and the TAX content was determined by LP MS (25 samples from 5 to 2100 min). The same volume of dissolution medium was replaced back after each sampling in order to maintain a constant volume and remain in sink conditions. Each release test was duplicated. The results are presented as kinetics of cumulative TAX release (in %) as a function of time:

$$\text{TAX released}\% \quad (Q_{r\ cumul}/Q_{ads}) * 100 \qquad (1)$$

where $Q_{r\ cumul}$ is the cumulative amount of TAX released and Q_{ads} is the initial quantity of TAX adsorbed.

2.5. Characterization of solids after adsorption

The solid phases before and after TAX adsorption were characterized by X ray diffraction (XRD), using an Equinox 1000 curved counter INEL diffractometer with a cobalt anticathode (λ_{Co} = 1.78892 Å). Raman microspectroscopy analysis was performed using a confocal microspectrometer (Horiba Jobin Yvon Labram HR800) with a helium neon laser (λ = 632.82 nm) over a wavenumber range of 350 1750 cm^{-1}. Transmission electron microscopy (TEM) micrographs were obtained on a JEOL JEM 2100F microscope set at an acceleration tension of 200 kV.

2.6. Hemostasis tests

Preliminary hemostatic tests were carried in this work by measuring the activated partial thromboplastin time (aPTT), which is a global screening assay to evaluate the coagulation cascade. The aPTT is the clotting time obtained when "partial thromboplastin" is added to plasma. Partial thromboplastin is the phospholipid fraction of a tissue extract and differs from a complete tissue extract (i.e., "thromboplastin") by the lack of tissue factor [18,19].

Blood specimens from 10 healthy adult dogs of various breeds were obtained by jugular venipuncture, using minimal restraint and hand compression. Blood specimens were drawn using a 0.8 × 25 mm needle (Neolus; Terumo Europe N.V., Leuven, Belgium) connected to a vacuum system (VenojectLuer adapter; Terumo Europe, N.V.) into a citrated tube (Venosafe; Terumo France, Guyancourt, France). Trisodium citrate (0.129 M) is a good calcium ligand, and in the ratio 1:9 (v/v), the decalcification prevents clot formation.

To examine the effect of two solid samples on the aPTT, 50 mg HA with and without adsorbed TAX (175 μmol TAX/g HA) was added to 1.2 mL of citrated whole blood, and the results were compared with the results obtained when only TAX was added (100 μL TAX in aqueous solution, 1 g/L). Citrated plasmas were then obtained after centrifugation of the blood specimens for 5 min at 2900 g (Hettich Rotofix 32 A, Tuttlingen, Germany).

aPTT was automatically measured using a STA Compact analyzer (Diagnostica Stago, Asnières sur Seine, France) after quality control using STA Coag Control N + P (Diagnostica Stago, Asnières sur Seine, France). Briefly, citrated plasma was incubated at 37 °C with an activator and phospholipid (partial thromboplastin). $CaCl_2$ was then added to start the coagulation cascade. Results are expressed in seconds, as the time taken for a fibrin clot to form. Each test was performed in duplicate.

3. Results and discussion

3.1. Characterization of powders

The synthesized HA sample had a Ca/P molar ratio of 1.66 ± 0.02 corresponding to stoichiometric hydroxyapatite ($Ca_{10}(PO_4)_6(OH)_2$). The specific surface area of HA was 58 (±3) m^2/g. The solids were characterized after adsorption. Its X ray diffraction pattern displayed characteristic diffraction lines of well crystallized hydroxyapatite and no

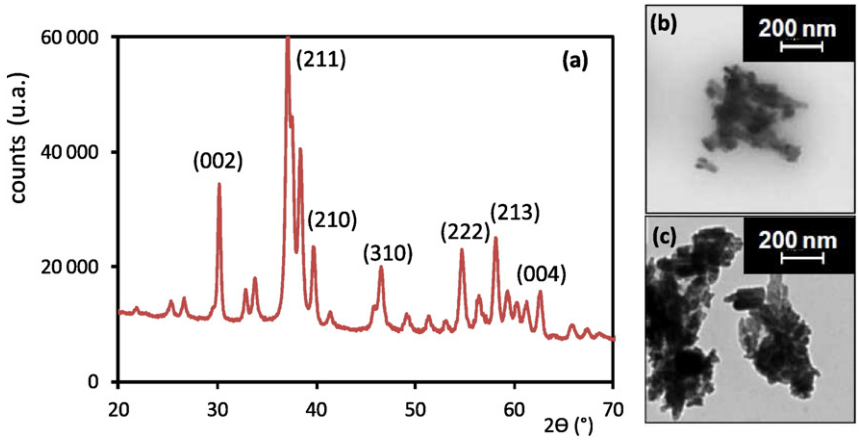

Fig. 3. (a) X-ray diffraction pattern of the powder sample after adsorption (HA-TAX) and indexation of the main diffraction lines in relation with JCPDS file ref. no.09–432. TEM observations of the powders (b) before (HA) and (c) after adsorption (HA-TAX), (175 μmol TAX/g HA).

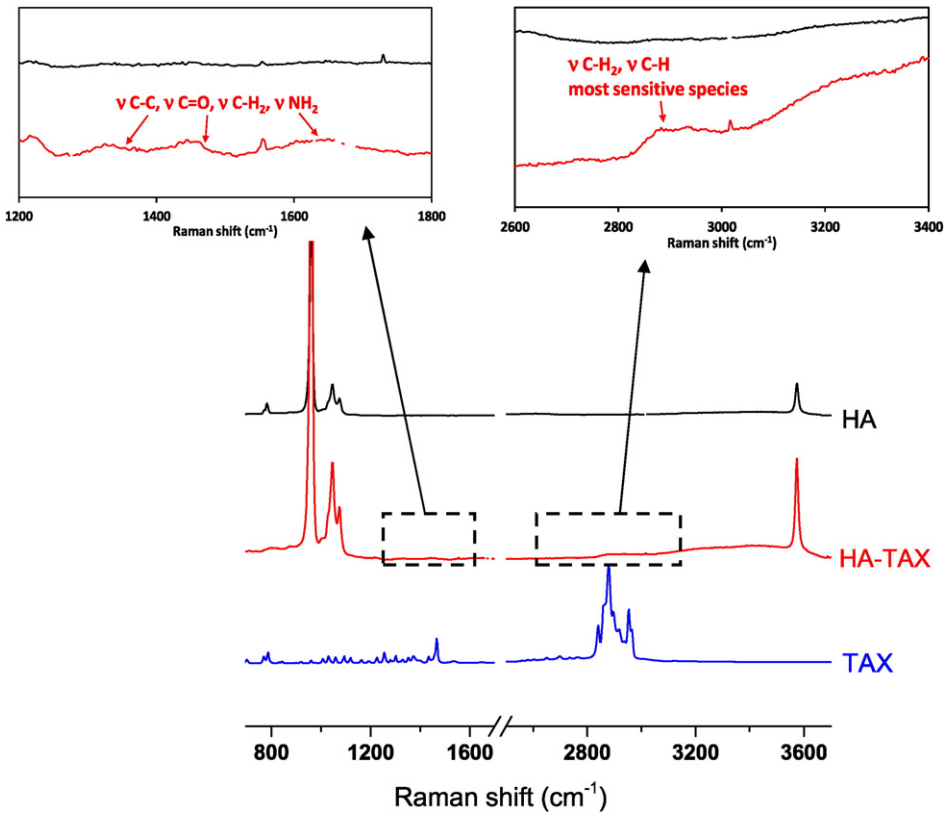

Fig. 4. Raman spectra of the samples before (HA) and after (HA-TAX) adsorption of tranexamic acid (TAX), (175 μmol TAX/g HA).

other crystalline phase was detected after TAX adsorption (Fig. 3a); these results were further confirmed by TEM. Furthermore, there was no apparent change in crystal size, as all crystals remained approxi mately 100 nm in length (Fig. 3b and c).

Raman spectra of the powders before (HA) and after (HA TAX) ad sorption are presented in Fig. 4 and compared with the Raman spectrum of pure TAX. Raman spectra of the solids showed characteristic lines of apatitic phosphate groups: ν_1 (960 cm^{-1}), ν_2 (430 450 cm^{-1}), ν_3 (1040 1074 cm^{-1}), and ν_4 (580 608 cm^{-1}) modes of PO_4^{3-} [20]. More over OH^- apatitic vibration was also detected around 3560 cm^{-1}. Char acteristic vibration bands corresponding to TAX around 1500 cm^{-1} (ν_{C-C}, $\nu_{C\ O}$, ν_{CH2}, ν_{NH2}), and between 2800 and 3000 cm^{-1} (ν_{CH2}, ν_{CH}), were slightly detected beside the HA spectrum after adsorption, probably because the amount of adsorbed TAX was limited and also be cause TAX molecule exhibits Raman vibration bands of low intensity.

3.2. Adsorption of tranexamic acid

The evolution of the amount of TAX adsorbed, Q_{ads} (μmol/m^2), on HA from dilute aqueous solutions (0 40 mM) as a function of its remaining concentration in solution, C_{eq} (mmol/L), is plotted in Fig. 5. As shown in the graph, no adsorption plateau was observed as the general tendency was a continuous increase of the adsorbed amount versus C_{eq}.

The adsorption of (bio)molecules with a strong affinity for apatite surfaces can often be described by the Langmuir isotherm [9]. This is the case for example for some biomolecules exhibiting phosphate or phosphonate endgroups as in phosphoserine or bisphosphonates. In this model, the solid surface is considered to be composed of energeti cally equivalent adsorption sites and no interaction exists between ad sorbate molecules [21,22] that form a monolayer on the surface of the substrate. Also, the adsorption of molecules exhibiting a high affinity for apatitic supports is often accompanied by a simultaneous ion ex change process, involving ions such as phosphate anions from the surface of apatite crystals. When the amount adsorbed on apatitic sur faces is small, the adsorption is generally more accurately described by the Freundlich model. This is the case for molecules such as glycine, acetic acid, or else serine [9,22]. Such molecules weakly interact with apatite surface due to the presence of endgroups that have only a low affinity for apatite surface, such as carboxylate. However, the present data give graphical evidence that TAX adsorption on HA cannot be de scribed by the Langmuir isotherm model or the Freundlich model. In deed, rather than a tendency toward stabilization, an increasingly greater adsorption versus C_{eq} is observed here. This evolution reminds a power law. Indeed, a mathematical analysis of the adsorption data

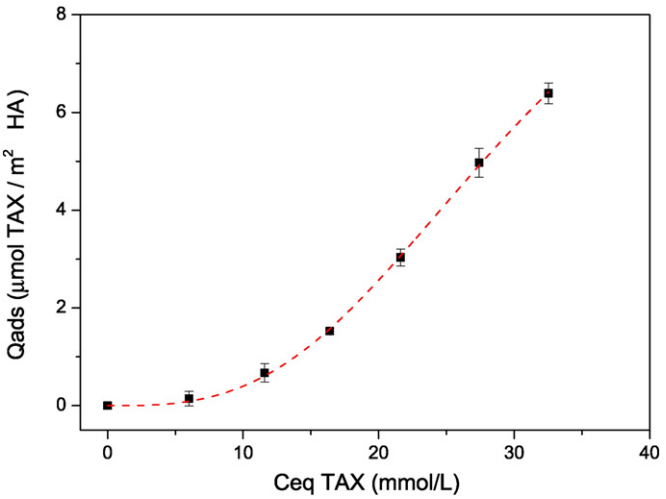

Fig. 5. Adsorption isotherm of TAX on HA at 37 °C.

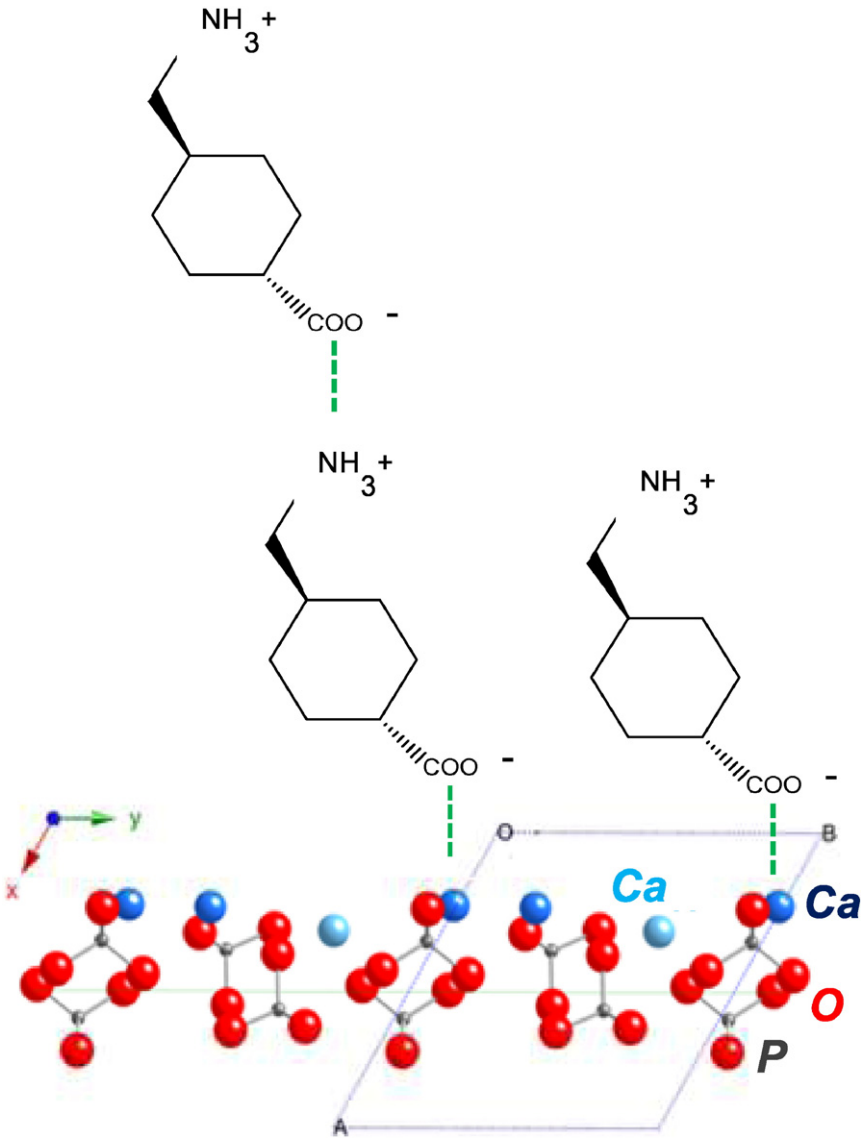

Fig. 6. Mechanism proposed for adsorption of TAX on the (001) surface plane of HA (using Crystalmaker and ChemDraw Softwares).

showed that the curve can be satisfactorily ($r^2 = 0.994$) described by an equation of the form:

$$Q_{ads} \quad K \times C_{eq}{}^{n} \tag{2}$$

with a value of "n" > 1, namely $n = 1.99 \pm 0.11$, and $K = 2.64 \pm 0.41$ (with Q_{ads} in μmol/m^2 and C_{eq} in mmol/L). Note that this equation should not be confounded with the one describing the typical Freundlich model which has an equivalent form but with an exponent "n" lower than 1.

At this point, it was also interesting to check how the adsorption data could mathematically be fitted with a Langmuir Freundlich equation, also known as Sips, which also affects an exponent to the equilibrium concentration, as in the equation:

$$Q_{ads} \quad N_m \times \frac{(K \times C_{eq})^{n}}{1 + (K \times C_{eq})^{n}} \tag{3}$$

(Note that there exists also an equivalent form of this equation that replaces K^n with the constant K_S). The mathematical treatment of the data showed that such an equation could indeed describe the evolution

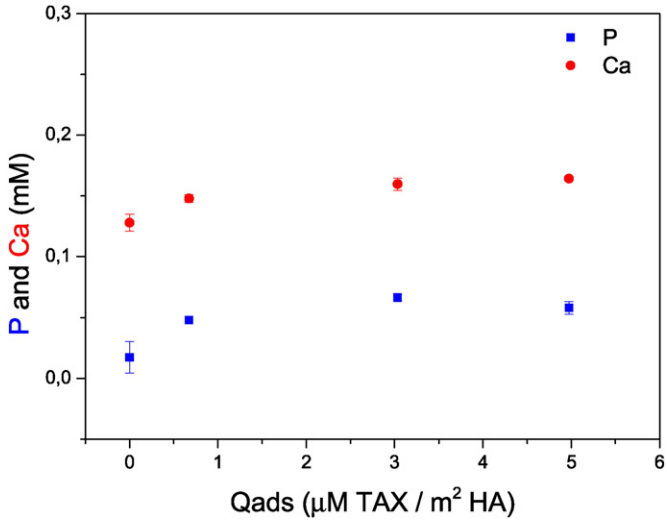

Fig. 7. Concentration of phosphate (*blue squares*) and calcium (*red circles*) ions in the solutions after adsorption upon Q_{ads} of TAX on HA.

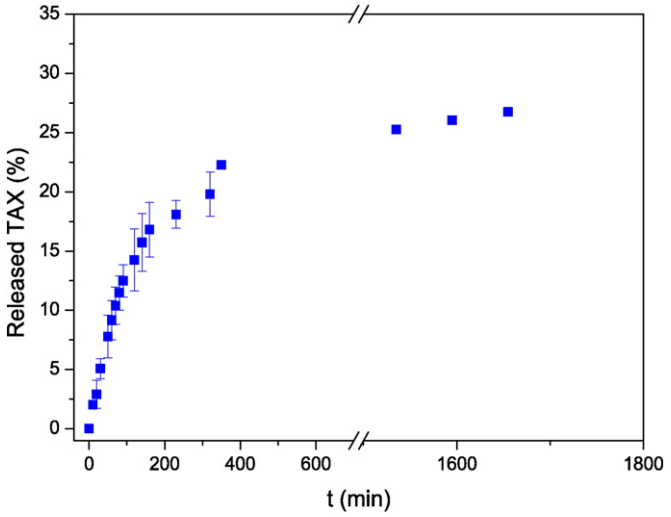

Fig. 8. Kinetics of release of TAX (%) from HA after adsorption. The amount of initial concentration of TAX was equal to Q_{ads} (TAX) = 175 μmol/g HA.

of Q_{ads} versus C_{eq} in the case of TAX adsorption on hydroxyapatite, with a correlation coefficient of $r^2 = 0.999$, and the parameters $n = 2.98 \pm 0.16$, $K = 0.032 \pm 0.002$ L/mmol, and $N_m = 11.85 \pm 1.14$ μmol/m^2. According to the Langmuir–Freundlich theory, departure from an ideal adsorption situation as depicted by Langmuir arises from the existence of surface heterogeneities with non equivalent sites and/or of non negligible interactions between adsorbed species. As previously mentioned in the literature, an exponent $n > 1$ suggests the existence of positive cooperativity between adsorbed molecules. Taking into account the shape of the isotherm observed here, the formation of multilayer of adsorbed molecules seems to be highly probable. The adsorbed amounts reached on the adsorption isotherm (Fig. 5) and by N_m value were both particularly high for molecules that do not expose high affinity groups for the surface of apatite surfaces. Indeed, only one carboxyl and one amino group are present on the TAX molecule, which present relatively low affinity for the surface of the apatite, as has been previously reported for example for the amino acid serine [22]. This was particularly true for the present apatite sample, which is stoichiometric and well crystallized, thus affected by a limited surface reactivity. In contrast, the adsorption of molecules such as bisphosphonates, for example, which exhibit high affinity phosphonate groups, led to maximum amounts adsorbed of approximately 3 μmol/m^2 on apatitic substrates [21]. The high adsorbed amounts observed here can only be explained by the formation of TAX multilayers, with molecules probably interacting with each other through respectively their $—COO^-$ and $—NH_3^+$ terminal groups. This is consistent with the exponent value found with the Langmuir–Freundlich model, suggesting a strong impact of intermolecular interactions rather than interactions with the surface of the nanocrystals. This is also consistent with the equilibrium dissociation constants of TAX from the literature (the pKa for carboxylic acid and amine functional groups in TAX were estimated to be 4.9 and 10.6, respectively [16]). The mechanism of interaction of TAX with HA could tentatively be then proposed in two steps: (1) TAX carboxyl groups interact with calcium ions on the surface of HA to form a mono layer on the apatitic support, and simultaneously (2) interaction between protonated amino groups and carboxyl species between adsorbate molecules of TAX leads to the formation of multilayers (Fig. 6). Note that the data were also tentatively fitted to other isotherm models often used to describe multilayer adsorption, including on solid samples, like the BET isotherm [23]. Although a moderately good fit was reached ($r^2 = 0.983$), the Langmuir–Freundlich still remained the best model to fit the experimental data.

3.3. Mineral ion composition of solutions after adsorption

The change in the mineral content of the solution is shown in Fig. 7. Note that there was no significant change in the pH of the solution during the adsorption experiments (pH remained close to 7.4). The data point related to a Q_{ads} equal to zero corresponded to a blank assay performed under the same conditions as the adsorption experiments in the absence of TAX. The calcium and phosphate ion content in the solution remained low (corresponding to low solubility of the HA substrate) and most importantly stable during the adsorption process, at approximately 0.15 and 0.05 mM, respectively, for calcium and phosphate. The mineral ion content in the solution therefore did not seem to be related to the amount of TAX adsorbed and was only due to the congruent dissolution of the crystals in aqueous solution as the Ca/P ratio in solution was the same as in the solid (i.e. Ca/P ~ 1.66). Therefore, the possibility of ion exchange occurring during the adsorption process can be ruled out, contrary to the case of several (bio)molecules with a strong affinity for the surface of apatites, as mentioned above.

3.4. Release kinetics

The kinetics of release of TAX (in %) from HA are shown in Fig. 8. The release was initially fast, as 20% of TAX was released during the first 6 h. Then TAX release slowed down, impacted by the dissolution of HA but not only. By linearization using different models, some linear zones can be pointed out allowing us to conclude that the release mechanism was probably governed by a complex process involving both diffusion (as in Korsmeyer–Peppas model for example) and dissolution (as in Hixson–Crowell model), as suggested by Fig. 9 [24,25].

3.5. Preliminary hemostasis results via aPTT evaluations

aPTT results are presented in Fig. 10. With regards to the solid samples, the aPTT of HA powders decreased for each specimen with the presence of adsorbed TAX. This can be clearly visualized by the lower position of the HA/TAX curve (*red circles*) as compared with the HA substrate alone (*black squares*).

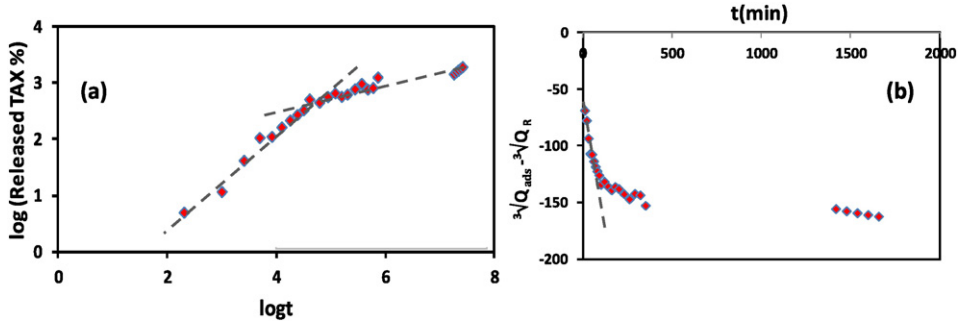

Fig. 9. Linear regression of (a) Korsmeyer–Peppas model (Release TAX% = $K_{KP} \times t^n$, with K_{KP} constant et n the diffusion parameter) and (b) Hixson–Crowell model ($\sqrt[3]{Q_{ads}} - \sqrt[3]{Q_R} = K_{HC} \times t$ with K_{HC} constant and Q_R the quantity of TAX released from HA) for the release kinetics of TAX from HA.

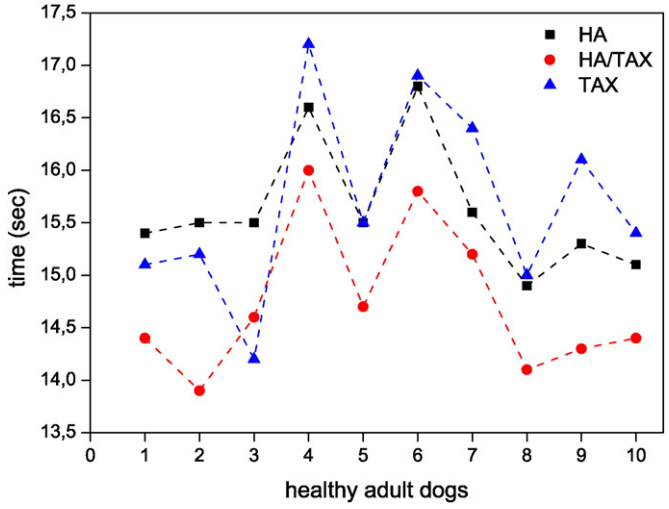

Fig. 10. aPTT obtained for the powders of hydroxyapatite before (HA) and after adsorption (HA/TAX with Qads (TAX) = 175 μmol/g HA), and for TAX solution (1 g/L) performed on ten healthy adult dogs.

Note that the data points corresponding to free TAX (blue triangles) relate to a solution while apatitic samples (HA and HA/TAX) were solids; therefore, the dilution of TAX during aPTT experiments prevented a direct comparison with the powder samples.

Although preliminary, these results point out a reduction in aPTT; this is extremely promising for the development of apatitic biomaterials with intrinsic hemostatic properties.

4. Conclusion

The aim of this work was to combine *tranexamic acid (TAX)*, a clini cally used antifibrinolytic agent, and hydroxyapatite (HA) widely used in bone replacement, to produce a novel bioactive apatitic biomaterial with intrinsic hemostatic properties. The study of the adsorptive behav ior of the TAX molecule onto HA was performed and its release in near physiological conditions was also followed. When the isotherm of ad sorption of TAX onto the HA surface was plotted, no adsorption plateau was observed as the general tendency was a continuous increase of the adsorbed amount. Despite the low affinity of TAX for the surface of HA crystals, likely due to the presence of only a carboxyl and an amino group known to have a relatively low affinity for the surface of apatite, significant adsorbed amounts could be reached: the adsorption data ex hibited an exponential tendency mathematically fitted to a Langmuir Freundlich equation with an exponent close to 3. This suggested a strong interaction between adsorbed molecules, resulting in the forma tion of multilayers. This tendency may be an advantage in practical he mostasis applications for potentially transporting large doses of TAX directly to the bleeding wound site for increased efficiency. Further more, it may be useful for adapting the dose of TAX to the condition of the patient (evaluation of bleeding risk, possible hemophilic condi tions…). The concentration of calcium and phosphate ions in solution remained low and stable during the adsorption process, thus ion ex change during the adsorption process can be ruled out. The release of TAX was fast during the first hours and was governed by a complex pro cess that likely involved both diffusion and dissolution of HA. The pre liminary hemostasis aPTT tests on the blood from ten healthy adult dogs showed promising results for the development of apatitic bioma terials with intrinsic hemostatic properties. Especially for surgical pro cedures known to present a high risk for bleeding, the search for improved hemostasis approaches or methodologies is still undergoing. One appealing approach when dealing with bone related surgeries is to confer hemostatic properties to the implanted biomaterial itself, and apatitic biomaterials appear well suited for this goal. This work con siders the possibility to develop apatitic based bone repair biomaterials with hemostatic activity and the preliminary results obtained are prom ising. This contribution can thus be seen as a first approach for the de velopment of osteoconductive and hemostatic biomaterials, which may be optimized in the future by the use of apatite nanoparticles allowing higher adsorbed amounts of drugs thanks to their larger spe cific surface areas and surface reactivity than HA, for further improving drug delivery properties.

References

[1] Dental Abstracts, 57 (2012) 307–308.
[2] A. Anne-Yvonne, B. Béatrice, Le Pharmacien Hospitalier, 43, Supplement 1 (2008) 2–8.
[3] D. Royston, Seminars in anesthesia, Perioperative Med. Pain 20 (2001) 18–23.
[4] C.M. Svahn, F. Merenyi, L. Karlson, J. Med. Chem. 29 (1986) 448–453.
[5] G. Hadad, A. El-Gindy, W.M. Mahmoud, Chroma 66 (2007) 311–317.
[6] C. Rey, C. Combes, C. Drouet, M. Glimcher, Osteoporos. Int. 20 (2009) 1013–1021.
[7] C. Drouet, F. Bosc, M. Banu, C. Largeot, C. Combes, G. Dechambre, C. Estournès, G. Raimbeaux, C. Rey, Powder Technol. 190 (2009) 118–122.
[8] C. Rey, C. Combes, C. Drouet, H. Sfihi, A. Barroug, Mater. Sci. Eng. C 27 (2007) 198–205.
[9] F. Errassifi, A. Menbaoui, H. Autefage, L. Benaziz, S. Ouizat, V. Santran, S. Sarda, A. Lebugle, C. Combes, A. Barroug, H. Sfihi, C. Rey, Adsorption on apatitic calcium phosphates: applications to drug delivery, in: R. Narayan, J. McKittrick (Eds.), Advances in Bioceramics and Biotechnologies, Amer Ceramic Soc, Westerville 2010, pp. 159–174.
[10] J. Gómez-Morales, M. Iafisco, J.M. Delgado-López, S. Sarda, C. Drouet, Prog. Cryst. Growth Charact. Mater. 59 (2013) 1–46.
[11] S. Ouizat, A. Barroug, A. Legrouri, C. Rey, Mater. Res. Bull. 34 (1999) 2279–2289.
[12] M. Iafisco, P. Sabatino, I.G. Lesci, M. Prat, L. Rimondini, N. Roveri, Colloids Surf. B: Biointerfaces 81 (2010) 274–284.
[13] T. Kawasaki, J. Chromatogr. A 544 (1991) 147–184.
[14] J.C. Trombe, UPS, Toulouse, France, 1972.
[15] G. Charlot, Chimie Analytique Quantitative, Masson et Cie ed, Paris, 1974.
[16] S. Grassin Delyle, E. Abe, A. Batisse, B. Tremey, M. Fischler, P. Devillier, J.C. Alvarez, Clin. Chim. Acta 411 (2010) 438–443.
[17] in: In: Europe Co. (Ed), European Pharmacopoeia 7th ed., (Strasbourg, France), 2011.
[18] M.R. Scola, L.M. Baggesen, T.C. Nichols, N.S. Key, C.M. Gallippi, Thrombosis research, 129, Supplement 2 (2012) S57–S61.
[19] E.J. Favaloro, G. Lippi, Thrombosis research, 127, Supplement 2 (2011) S13–S16.
[20] D. Eichert, C. Drouet, H. Sfihi, C. Rey, C. Combes, Biomaterials Research Advances 93, 2008.
[21] P. Pascaud, P. Gras, Y. Coppel, C. Rey, S. Sarda, Langmuir 29 (2013) 2224–2232.
[22] L. Benaziz, A. Barroug, A. Legrouri, C. Rey, A. Lebugle, J. Colloid Interface Sci. 238 (2001) 48–53.
[23] K.Y. Foo, B.H. Hameed, Chem. Eng. J. 156 (2010) 2–10.
[24] S. Dash, P.N. Murthy, L. Nath, P. Chowdhury, Acta Pol. Pharm. 67 (2010) 217–223.
[25] P. Costa, J.M. Sousa lobo, Eur. J. Pharm. Sci. 13 (2001) 123–133.